International Journal of Modern Manufacturing Technologies
ISSN 2067–3604, Vol. XIV, No. 1 / 2022
https://doi.org/10.54684/ijmmt.2022.14.1.75

SURFACE IMPROVEMENT OF AISI D3 STEEL EMPLOYING SiC BLENDED DIELECTRIC IN ELECTRIC DIE SINKING PROCESS

Santarao Korada[1], Munmun Bhaumik[2], Prasad C L V R S V[1]

[1]Department of Mechanical Engineering, GMR Institute of Technology, Rajam, India, 532127,
[2]Department of Mechanical Engineering, G V P College for Degree and PG Courses, Visakhapatnam, India, 530045

Corresponding author: Santarao Korada, santarao.k@gmrit.edu.in

Abstract: AISI D3 die steel is extensively used in long-run dies for blanking, forming, deep drawing, and thread rolling. Among all the non-traditional machining processes, the Electric Die Sinking Process (EDSP) is mostly employed to manufacture these long-run dies. The EDSP method produces a surface of high quality, which impacts product performance significantly. The surface roughness of AISI D3 die steel is examined in relation to a number of parameters, including peak current, pulse-on duration, gap voltage, and powder concentration. Copper is selected as the tool. Orthogonal array concept coined by Taguchi has been deployed to execute the experiments. It is clearly understood from the results that powder concentration has a key impact on machined surface quality by lessening the generated cracks and enhancing the surface finish by 20%. Further, peak current has more impact on the performance characteristics than pulse-on time and the gap voltage.

Keywords: AISI D3 die steel, Micro cracks, Surface Roughness, Taguchi methodology, Electric Die Sinking Process (EDSP)

1. INTRODUCTION

Electric Die Sinking Process (EDSP) is used to machine micro-size; die and mould materials; specific micro-featured tools and components; and intricate shapes without considering the hardness of the material (Prihandana et al., 2009; Jahan et al., 2010; Prihandana et al., 2011). This method is governed by controlled thermal erosion of electrically conductive material's surface that is immersed in dielectric (Santarao et al., 2017). This machining approach is currently implemented in automotive, press tools, aerospace industries along with surgical equipment manufacturing companies (Kumar et al., 2010). Various approaches, such as powder mixed/suspended dielectric fluid; vibrated tool/workpiece; and rotated tool, have been used to increase machining efficiency in EDSP (Prihandana et al., 2009). Among all methods mentioned, the first method has more capability to impart functional properties and amplify surface quality of the machined surface which is known as Powder Mixed Electric Die Sinking Process (PMEDSP) (Tan and Yeo, 2011). In contrast to traditional EDM, powder blended dielectric based EDSP has a diverse method of machining. An electrical field in the range 105-107 V/m is created when 80-320 V is applied in 25-50 microns gap between the tool and the work component. This enhances the energy of powder particles and enable them to come close to one another and settle down in a cross-series fashion. This series configuration allows to reduces gap between the two electrodes connected. Due to the linkage effect, the dielectric fluid loses its insulating strength. As a result, premature explosion happens in the gap. The fine grain powder used affects the plasma channel (expands and enlarges). The spark is therefore disbursed uniformly among powdered particles; the density of the spark therefore decreases. The homogeneous sparking distribution of the powdered particles contributes to the formation of shallow craters on the outside surface of the workpiece. The surface finish will be enriched.

Spark energy and peak current increased the surface roughness of Nimonic C-263 while spark frequency had the opposite effect (Bisaria and Shandilya, 2019). When machining Alloy steel 20MnCr5, all response characteristics were affected by peak current and pulse-on time (Kumar and Goyal, 2020). When using MoS_2 powder with particle sizes of 10nm, 50nm, and 2μm suspended in kerosene to fabricate 300μm blind holes on Inconel 718, high material removal rates were achieved for 50nm (Prihandana et al., 2014). Again, they published the results obtained after suspending Gr powder (~55nm) into kerosene, when machining 50μm deep blind holes on silver-tungsten using a 300μm cylindrical tool electrode at a feed rate of 5μm/s. They noticed that surface quality of machined surface was enriched by eliminating micro-cracks and the average surface finish improved by 78% (Prihandana et al., 2011). At 0.2 g/l concentration and 60V electrical setting, machining WC with Gr (55nm) mixed in ELF EDM3 oil resulted in a good surface finish (Jahan et al., 2011). Again, they presented the effects of adding Al (~18nm), Al_2O_3 (~25nm) and Gr (~55nm) into EDM3 Oil during μ-EDSP operation. Sinking and milling operations were performed on tungsten carbide using a 500μm diameter tool electrode at different powder concentrations ranging from 0.03-2.0 g/l. They found that semi-conductive Gr nano powder provides a smooth and shiny surface. Higher material removal rate (MRR) was achieved when aluminum was used, but non-conductive alumina had little effect on the EDSP performance (Jahan et al., 2010). The average surface finish improved by 76-86% compared to the pure dielectric when mixing Al_2O_3 (~45-55nm) powder into the Daphene Cut HL25-S oil during μ-EDSP operation (Tan et al., 2008). A considerable enrichment in surface topography of the machined surface was observed when Al_2O_3 powder (~45-50nm) mixed dielectric in traditional EDSP (Kumar et al., 2018). The surface finish of steel was improved by the addition of Al_2O_3 powder (Saravanakumar et al., 2018). Results of nano aluminium PMEDSP on titanium alloy material show slight improvement in terms of surface roughness and surface morphology as compared to conventional EDSP (Abdul-Rani et al., 2017). Material removal rate and surface finish improved by 69 percent and 35 percent, respectively, when machining D2 die steel with Ti powder (40-60nm) mixed with hydrocarbon oil (Marashi et al., 2015). Performing machining on D3 die steel with a 50nm SiC powder blended dielectric has significantly improved material removal and reduced tool wear (Santarao, et al., 2018). A glimpse of the literature reviewed is presented in Table 1.

Table 1. Properties of powder used in powder-mixed EDSP

Powder	Thermal Conductivity (W/cm K)	Density (g/cm^3)	Size (nm)	Reference
Al_2O_3	0.35	3.89	25, 45-55	Tan et al., 2008; Jahan et al., 2010; Kumar et al., 2018; Saravanakumar et al., 2018
MoS_2	1.38	5.06	10, 50 & 2000	Prihandana et al., 2014
Gr	1.5	2.23-2.25	55	Prihandana et al., 2011 Jahan et al., 2010; Jahan et al., 2011
Al	2.38	2.70	18	Jahan et al, 2010; Abdul-Rani et al., 2017
Ti	-	-	40-60	Marashi et al., 2015
SiC	3.0	3.21	50	Santarao, et al., 2018

From Table 1, based on nano powder mixed EDSP, it is understood that earlier researchers concentrated on powders with thermal conductivity (TC) in the range between 0.35 W/cmK and 2.38 W/cmK. Thermal conductivity plays a vital role that affects the surface quality in powder mixed EDSP process Fong and Chen, 2005; Talla et al., 2016). Therefore, a gap in the literature for usage of a powder with higher thermal conductivity (TC) is less explored has been observed. Hence, in this study powder with higher TC is added in the dielectric fluid and Taguchi L9 OA has been adopted to conduct the experiment on AISI D3 die-steel using copper electrode during EDSP operation. The purpose of this research is to determine the impact of SiC powder concentration and other process variables listed in Table 2 on surface roughness (SR) of PMEDSPed AISI D3 die-steel. Microstructural analysis has been performed.

2. EXPERIMENT SET-UP AND METHOD

2.1 Process variables and Response

For this study, process variables as listed in Table 2 are considered and surface roughness (SR) is selected as a response parameter. Process variables, those have substantial effect on the EDSP performance characteristics are selected as evident from the literature. The range of the processing parameters have been chosen in such a way that the machining operation come under the semi finishing category. Table 2 shows the Process variables and levels.

Table 2. Process variables and levels

Process variable	Levels		
	Level 1	Level 2	Level 3
Pulse-on time, T_{on}, (μs)	50	100	150
Peak current, I_p, (A)	5	6	7
Powder concentration, P_C, (g/l)	0	0.5	1
Gap voltage, V_g, (V)	50	60	70

2.2 Experiment set-up

The experiments were performed on S-50 ZNC model electrical discharge machine (EDM) procured from ELECTRONICA MACHINE TOOLS. A novel experimental set-up for nanopowder mixed EDSP (NPMEDSP) is devised in order to limit the quantity of dielectric needed and to prevent damage to the available filtering arrangement owing to settling of nanopowder in filters. Figure 1 depicts the new fabricated set-up. It comprises of a 10lts container with a motorised stirrer and dielectric recirculating pump, a dielectric source tank with magnets, and a centrifugal pump. In addition, a PVC ball operating valve is used to control the flow of fluid in the piping system. An in-line venturimeter meter is used to check the flow speed.

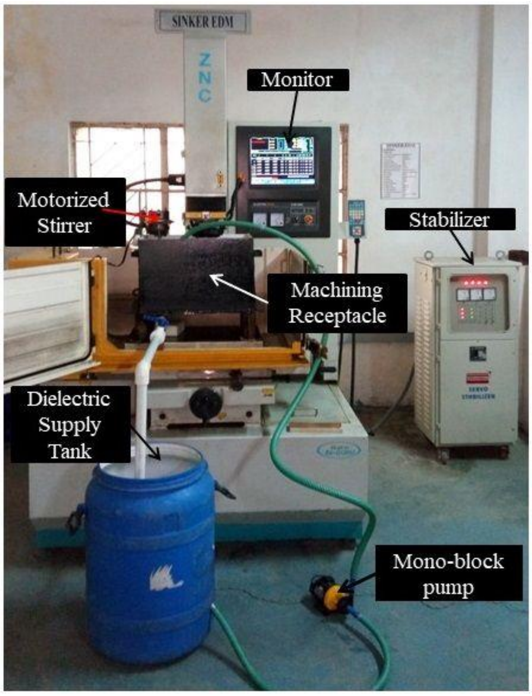

Fig. 1. PMEDSP Set-up

2.3 Workpiece, Tool, and powder material

In this investigation, AISI D3 die steel having dimensions 32.5mm×45mm×12mm and copper rod having dimensions 150mm×ϕ9.5mm respectively are selected as workpiece and tool. AISI D3 die Steel hardness ranges from 54 to 61 HRC. It has low machinability (Serope and Steven R., 2002). Chemical composition of workpiece is presented in Table 3. SiC powder of ~50nm size with TC 3W/cm K is selected in the present investigation.

Table 3. Chemical composition of as-received AISI D3 Steel

Element	Weight (%)
Carbon (C)	2-2.3
Manganese (Mn)	0.6
Sulfur (S)	0.03
Silicon (Si)	0.6
Phosphorous (P)	0.03
Chromium (Cr)	11-13.5
Molybdenum (Mo)	0.08
Iron (Fe)	Balance

2.4 Performance evaluation and measuring equipment

Surface roughness is calculated according to equation presented in (1).

$$R_a = \frac{1}{L}\int_0^L |f(z)dz| \quad (1)$$

where *f(z)* is the profile height function, and L is evaluation length that equals to hole diameter. It is measured along horizontal and vertical diameters on the machined surface with Mitutoyo make (SJ-201) surface roughness tester and the average value is considered for analysis. The detailed procedure of measuring the surface roughness is detailed in the previous article published by the author (Santarao, et.al, 2019).

2.5 Experiment plan

Each process variable is set to three levels as shown in Table 2. The Taguchi method is utilized to plan and conduct the experiments. Taguchi L9 orthogonal array, which consists of nine sets of process variable value combinations was selected (Ranjit K, 2010). Experiments designed using standard orthogonal array is presented in Table 4. Each machining set was performed for 20min and repeated three times. The recorded surface roughness is presented in Table 4. Figure 2 depicts a machined workpiece considering 4th combination from Table 4.

Table 4. Orthogonal array experimental design

Experiment Trail	Levels				Surface Roughness (μm)	
	I_p	T_{on}	V_g	P_C	MHD	MVD
1	5	50	50	0	6.910	6.240
2	5	100	60	0.5	4.550	4.550
3	5	150	70	1	5.030	5.180
4	6	50	60	1	4.570	4.690
5	6	100	70	0	4.690	4.420
6	6	150	50	0.5	4.850	4.590
7	7	50	70	0.5	5.000	4.950
8	7	100	50	1	5.040	4.900
9	7	150	60	0	6.570	6.610

Note: MHD, MVD represent measurement along horizontal and vertical diameters.

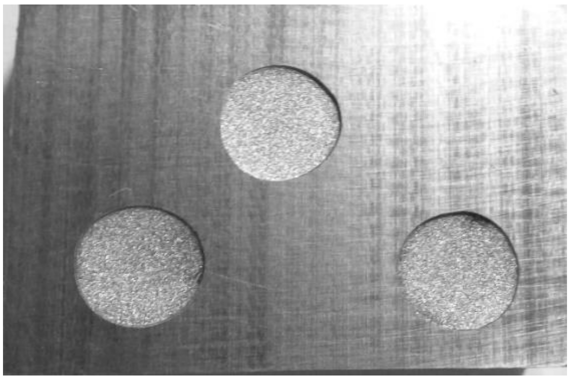

Fig. 2. Blind holes fabricated at trail 4

3. RESULTS AND DISCUSSION

The entire section is divided into five sub-sections. In the first four sub-sections, a detailed discussion on effect of each process parameter on surface roughness is presented. The fifth sub-section deals with the effect of added powder on surface cracks.

3.1. Powder concentration impact on surface roughness

From Figure 3, it can be inferred that at 0.5 g/l powder concentration, surface roughness significantly decreased by around 20%. This development in SR at 0.5 g/l is because when powder is blended into dielectric the plasma channel enlarges and widens.

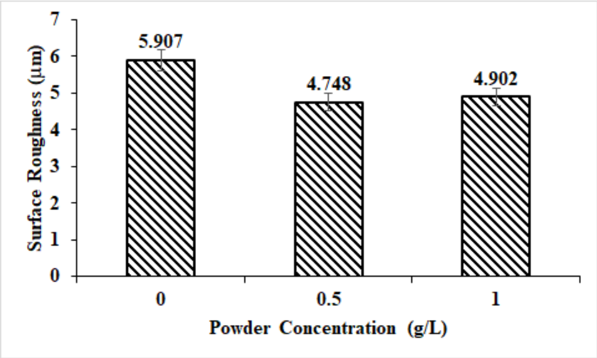

Fig. 3. Variation of surface roughness with powder concentration

As a result, the density of electric sparks decreases when sparks are distributed evenly among powder particles. Subsequently, craters to a shallow depth form on the workpiece surface (Jahan et al., 2010). On the other hand, 1 g/l powder concentration leads 3% surge in surface roughness. At more concentration, powder settlement is a common issue as such dielectric loses its capacity to spread the powder evenly. As a result, powder particles bridge themselves. The frequency of short-circuiting and arcing increases. This powder particle bridging leads in intensified discharge energy and carbon formed gets accumulated on the workpiece surface. Consequently, surface finish deteriorates (Jahan, Rahman and Wong, 2010; Kumar and Davim, 2011).

3.2. Impact of peak current on surface roughness

From Figure 4, it is evident that a rise in the surface roughness by 14% and 1% is observed when the peak current was increased from 5A to 6A, and 6A to 7A respectively. This is because when peak current increases, the spark energy expands, causing a force on the workpiece surface. This force expels more volume of material in molten form and generates bigger cavities, thus intensifies the surface irregularities (Syed and Palaniyandi, 2012).

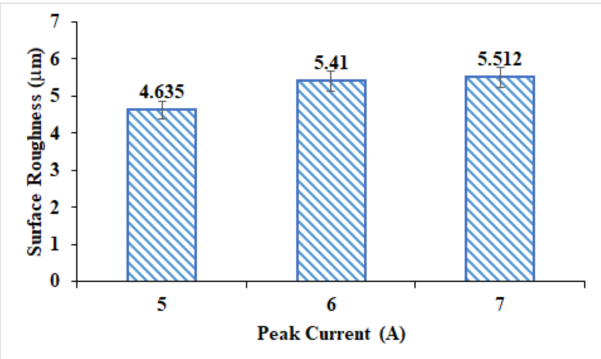

Fig. 4. Variation of surface roughness versus peak current

3.3. Impact of pulse-on time on surface roughness

As obvious from Figure 5, a 12% improvement in surface roughness was observed at 100µs. This decreasing trend in surface roughness from 50µs to 100µs is because of low pulse durations that lead to less vaporization of workpiece surface. Further, upon increase in the pulse-on time from 100µs to 150µs an increment of 14% in the surface roughness is observed. At a fixed current, a variation in pulse on-time results in a proportionate intensification in spark energy and subsequently, the melting boundary develops deeper and wider. Thus, it increases the roughness value. This type of variation was also observed by Syed et al. (Syed and Palaniyandi, 2012) .

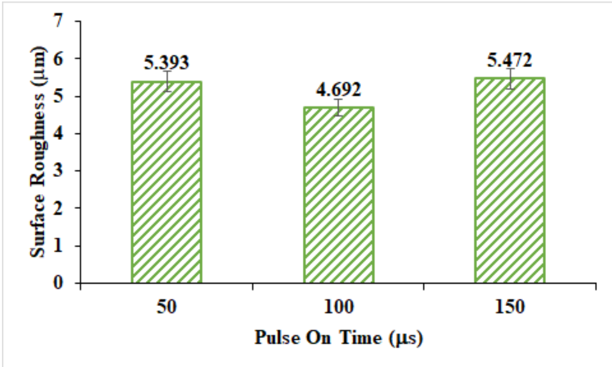

Fig. 5. Variation of surface roughness versus pulse-on time

3.4. Influence of gap voltage on surface roughness

As observed in Figure. 6, when the gap voltage was increased from 50 V to 60 V, the surface roughness decreased by 3%. In addition, further decrease in surface roughness of about 7% was observed when gap voltage was increased from 60 V to 70 V. This is because when the gap voltage grows, so does the inter-electrode gap. As the IEG increases, the spark frequency reduces and less depth of surface layer is vaporized leading to decrease in surface roughness. This observation complies with the work conducted by Singh et al. (Singh et al., 2010).

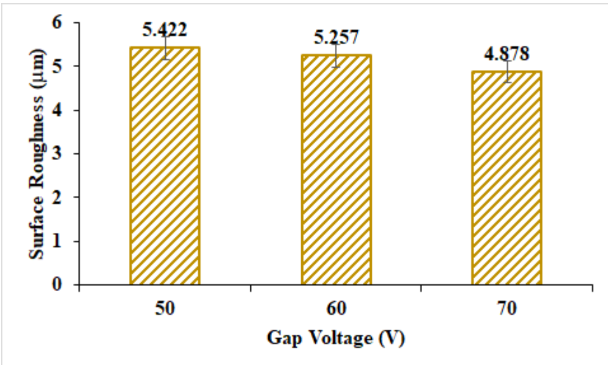

Fig. 6. Variation of surface roughness with gap voltage

3.5 Effect of powder concentration on surface texture

Figures 7 and 8 show SEM images of PMEDSed surfaces with unblended dielectric and SiC powder blended dielectric. These images are captured employing a SEM machine of JEOL MAKE – JSM6510LV at a working distance (WD) of 12mm and at 1000X magnification. As SiC nanopowder added into the dielectric, micro-cracks appeared less on the surface shown in Figure 8. This is due to the fact that, in PMEDSP, heat remaining in the sparking neighborhood is carried away by the added powder. As a result, reduced plasma channel pressure enables uniform energy dissemination and slow cooling of the molten metal. Hence, less micro-cracks formation is observed (Jahan, Rahman and Wong, 2011).

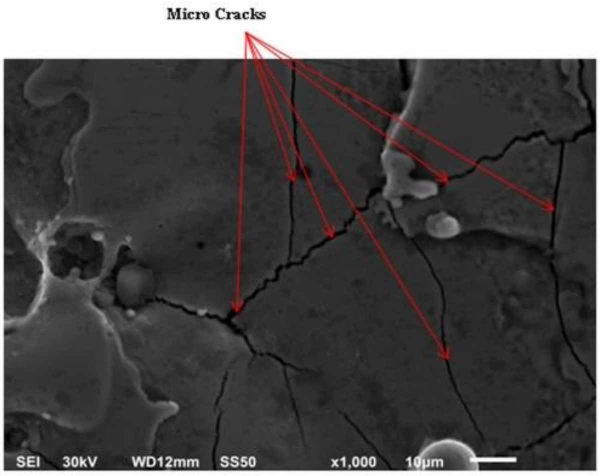

Fig. 7. Micro-cracks on the surface machined with un-blended dielectric

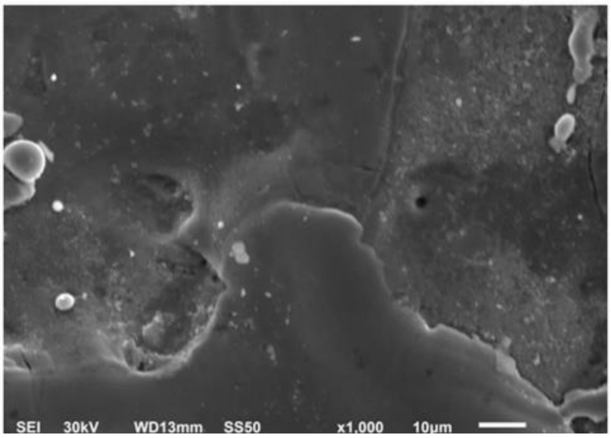

Fig. 8. Micro-cracks on the surface machined with blended dielectric

4. CONCLUSION

In this presented work, effect of peak current, pulse-on duration & gap voltage along with SiC powder (~50nm) concentration on the surface roughness is reported during EDSP of AISI D3 steel. The work yields the following conclusions:

1. It was observed that surface roughness reduced significantly up to 20%, 14%, 12% and 3% - 7% when powder particles added up to 1 g/l, peak current varies from 5 A to 7 A, pulse-on time varies from 50 µs to 150 µs and gap voltage varies from 50 V to 70 V respectively. Hence it is defended that powder addition is the most influencing variable. Peak current & pulse-on duration are another foremost influencing variable on SR. Effect of gap voltage on SR is very less.
2. Degree of surface quality enhanced using SiC nanopowder into the dielectric compared to conventional EDSP.

5. REFERENCES

1. Abdul-Rani, A. M., Nanimina, A. M., Ginta, T. L. and Razak, M.A., (2017). *Machined Surface Quality in Nano Aluminum Mixed Electrical Discharge Machining*. Procedia Manuf., 7, pp. 510–517.

2. Bisaria, H. and Shandilya, P., (2019). *Experimental investigation on wire electric discharge machining (WEDM) of Nimonic C-263 superalloy*. Mater. Manuf. Process., 34(1), pp. 83–92.

3. Jahan, M. P., Rahman, M. and Wong, Y. S., (2010). *Modelling and experimental investigation on the effect of nanopowder-mixed dielectric in micro-electrodischarge machining of tungsten carbide*. Proc. Inst. Mech. Eng. Part B J. Eng. Manuf., 224(11), pp. 1725–1739.

4. Jahan, M. P., Rahman, M. and Wong, Y. S., (2011). *Study on the nano-powder-mixed sinking and milling micro-EDM of WC-Co*. Int. J. Adv. Manuf. Technol., 53(1–4), pp. 167–180.

5. Kumar, A., Maheshwari, S., Sharma, C. and Beri, N., (2010). *A study of multiobjective parametric optimization of silicon abrasive mixed electrical discharge machining of tool steel*. Mater. Manuf. Process., 25(10), pp. 1041–1047.

6. Kumar, A., Mandal, A., Dixit, A. R. and Das, A. K., (2018). *Performance evaluation of Al_2O_3 nano powder mixed dielectric for electric discharge machining of Inconel 825*. Mater. Manuf. Process., 33(9), pp. 986–995.

7. Kumar, H. and Davim, J.P., (2011). *Role of Powder in the Machining of Al-10%Sicp Metal Matrix Composites by Powder Mixed Electric Discharge Machining*. J. Compos. Mater., 45(2), pp. 133–151.

8. Kumar, N. and Goyal, K., (2020). *Multi-objective optimization of wire electrical discharge machining of 20MnCr5 alloy steel*. World J. Eng., 17(3), pp. 325–333.

9. Marashi, H., Sarhan, A.A.D. and Hamdi, M., (2015). *Employing Ti nano-powder dielectric to enhance surface characteristics in electrical discharge machining of AISI D2 steel*. Appl. Surf. Sci., 357, pp. 892–907.

10.Prihandana, G.S., Mahardika, M., Sambo, S. A. R., Hamdi, M., Wong, Y. S. and Mitsui, K., (2009). *Workpiece vibration aided nano-graphite powder suspended dielectric fluid in micro-electrical*

discharge machining (μ-EDM) processes. In: *Proceedings of the 5th International Conference on Leading Edge Manufacturing in 21st Century, LEM*. pp. 3–8.
11. Prihandana, G.S., Mahardika, M., Hamdi, M., Wong, Y. S. and Mitsui, K., (2011). *Accuracy improvement in nanographite powder-suspended dielectric fluid for micro-electrical discharge machining processes*. Int. J. Adv. Manuf. Technol., 56(1–4), pp. 143–149.
12. Prihandana, G. S., Sriani, T., Mahardika, M., Hamdi, M., Miki, N., Wong, Y. S. and Mitsui, K., (2014). *Application of powder suspended in dielectric fluid for fine finish micro-EDM of Inconel 718*. Int. J. Adv. Manuf. Technol., 75(1–4), pp. 599–613.
13. Ranjit K, R., (2010). *A Primer on the Taguchi Method*. 2nd ed. Society of Manufacturing Engineers.
Santarao, K., L. V. R. S. V. Prasad, C. and Swaminaidu, G., (2017). *Influence of Nano and Micro Powders in Electric Discharge Machining: A Review*. J. Manuf. Technol. Res., 8(1–2), pp. 11–20.
14. Santarao, K., L. V. R. S. V. Prasad, C. and Naidu, G. S., (2018). *Experimental investigation on influence of SiC nanopowder blended dielectric in electric spark machining*. Int. J. Mod. Manuf. Technol., 10(1), pp. 84–91
15. Santarao, K., L. V. R. S. V. Prasad, C. and Swaminaidu, G., (2019). *Influence of dominant variables and their optimization for nanopowder blended EDM process*. Indian J. Eng. Mater. Sci., 26(October-December), pp. 356–362.
16. Saravanakumar, A., Santarao, K. and Nandini, G., (2018). *Influence of alumina nano powder mixed dielectric fluid in electric spark machining of aisi D3 steel*. Int. J. Mech. Prod. Eng. Res. Dev., 8(2), pp. 1257–1264.
17. Serope, K. and Steven R., S., (2002). *Manufacturing Engineering and Technology*. 4th ed. Delhi: Pearson Education Asia.
18. Singh, P., Kumar, A., Beri, N. and Kumar, V., (2010). *Influence of Electrical Parameters in Powder Mixed Elecric Discharge Machining (PMEDM) of Hastelloy*. J. Eng. Res. Stud., 1(2), pp. 93–105.
19. Syed, K.H. and Palaniyandi, K., (2012). *Performance of electrical discharge machining using aluminium powder suspended distilled water*. Turkish J. Eng. Environ. Sci., 36(3), pp. 195–207.
20. Talla, G., Gangopadhyay, S. and Biswas, C.K., (2016). *Effect of powder-suspended dielectric on the EDM characteristics of Inconel 625*. J. Mater. Eng. Perform., 25(2), pp. 704–717.
21. Tan, P.C. and Yeo, S.H., (2011). *Investigation of recast layers generated by a powder-mixed dielectric micro electrical discharge machining process*. Proc. Inst. Mech. Eng. Part B J. Eng. Manuf., 225(7), pp. 1051–1062.
22. Tan, P. C., Yeo, S. H. and Tan, Y. V, (2008). *Effects of Nanopowder Additives in Microelectrical Discharge Machining*. Int. J. Precis. Eng. Manuf., 9(3), pp. 22–26.
23. Yih-Fong, T. and Fu-Chen, C., (2005). *Investigation into some surface characteristics of electrical discharge machined SKD-11 using powder-suspension dielectric oil*. J. Mater. Process. Technol., 170(1–2), pp. 385–391.

Received: March 30, 2022 / Accepted: June 15, 2022 / Paper available online: June 20, 2022